IOPscience iopscience.iop.org

Home Search Collections Journals About Contact us My IOPscience

Magnetic properties of $Ho_{3-x}Y_xCu_4Sn_4$ (x = 0, 1, 2)

This article has been downloaded from IOPscience. Please scroll down to see the full text article.

2008 J. Phys.: Condens. Matter 20 295205

(http://iopscience.iop.org/0953-8984/20/29/295205)

View the table of contents for this issue, or go to the journal homepage for more

Download details:
IP Address: 129.252.86.83
The article was downloaded on 29/05/2010 at 13:34

Please note that terms and conditions apply.

J. Phys.: Condens. Matter **20** (2008) 295205 (6pp) doi:10.1088/0953-8984/20/29/295205

Magnetic properties of $Ho_{3-x}Y_xCu_4Sn_4$ ($x = 0, 1, 2$)

Ł Gondek[1], A Arulray[2], S Baran[3], K Nenkov[4,5], B Penc[3], A Szytuła[3,6] and K Tomala[3]

[1] Faculty of Physics and Applied Computer Science, AGH University of Science and Technology, Mickiewicza 30, 30-059 Kraków, Poland
[2] BENSC, Hahn-Meitner-Institute, Glienicker Street 100, 14 109 Berlin-Wannsee, Germany
[3] M Smoluchowski Institute of Physics, Jagiellonian University, Reymonta 4, 30-059 Kraków, Poland
[4] Leibnitz-Institute for Solid State and Materials Research, PO Box 270116, D-01 171 Dresden, Germany
[5] International Laboratory of High Magnetic Fields and Low Temperatures, Gajowicka 95, 53-529 Wrocław, Poland

E-mail: szytula@if.uj.edu.pl

Received 24 January 2008, in final form 5 June 2008
Published 26 June 2008
Online at stacks.iop.org/JPhysCM/20/295205

Abstract

X-ray and neutron diffraction, isothermal magnetization, magnetic susceptibility and specific heat measurements were performed on polycrystalline samples of $Ho_{3-x}Y_xCu_4Sn_4$ for $x = 0$, 1, 2. All samples crystallize with the orthorhombic structure of $Gd_3Cu_4Ge_4$ type. Within this crystal structure the rare earth atoms occupy two non-equivalent 2d and 4e positions. The presented x-ray data clearly indicate that introduced yttrium atoms prefer the 4e sublattice. Increase of the yttrium content causes a decrease of the Néel temperature from 7.6 K for $x = 0$ down to about 1.5 K for $x = 2$. Neutron diffraction data indicate that only Ho magnetic moments within the 2d sublattice order antiferromagnetically. The Ho moments are parallel to the b-axis. They form a collinear magnetic structure with the propagation vector $k = (0, 1/2, 0)$ with [++] sign sequence.

Dedicated to Professor Janusz Leciejewicz on the occasion of his 80th birthday.

1. Introduction

$R_3T_4X_4$, where R is a rare earth element, T is a transition metal and X = Si, Ge, Sn, are a very interesting group of compounds. These compounds crystallize in the orthorhombic $Gd_3Cu_4Ge_4$-type crystal structure (space group $Immm$) [1]. The unit cell contains two formula units and the rare earth atoms occupy two different sublattices (2d and 4e). For a certain number of compounds magnetic measurements have indicated very complex magnetic properties [2–19]. According to our recent findings based on analyses of complementary experimental data, some compounds exhibit independent ordering of the rare earth magnetic moments on both sublattices [17–19]. Namely, the 2d and 4e sublattices order at different temperatures. Moreover, they exhibit different types of propagation vectors and anisotropy.

For $Ho_3Cu_4Sn_4$, magnetic and neutron diffraction data indicate multiple magnetic phase transitions taking place at 2.3, 3.2, 4.4, 5.5 and 7.6 K [4, 18]. Results presented in these works indicate independent magnetic ordering on both sublattices. To explain this intriguing phenomenon, samples of $Ho_{3-x}Y_xCu_4Sn_4$ ($x = 0$, 1 and 2) composition were synthesized. In these samples magnetic moments are localized only on the Ho atoms. A substitution of the Ho atoms by non-magnetic Y ones was made to gain information on the magnetic properties on different sublattices. Further increase of the Y content ($Y_3Cu_4Sn_4$) leads to establishing the Pauli paramagnet [20]. In this work, results of x-ray and neutron diffraction, magnetic and specific heat measurements are presented.

2. Experimental details

Polycrystalline samples of $Ho_{3-x}Y_xCu_4Sn_4$ ($x = 0$, 1 and 2) were obtained by arc melting of stoichiometric amounts of

[6] Author to whom any correspondence should be addressed.

 © 2008 IOP Publishing Ltd Printed in the UK

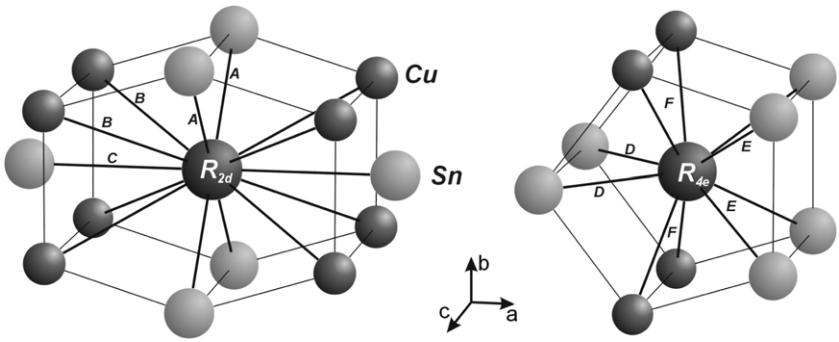

Figure 1. Coordination of the rare earth 2d and 4e positions. Interatomic distances between the rare earth and its nearest neighbours are labelled with capital letters ($A = R_{\mathrm{Ho2d-Sn4h}}$; $B = R_{\mathrm{Ho2d-Cu8n}}$; $C = R_{\mathrm{Ho2d-Sn4f}}$; $D = R_{\mathrm{Ho4e-Sn4f}}$; $E = R_{\mathrm{Ho4e-Sn4h}}$; $F = R_{\mathrm{Ho2d-Cu8n}}$).

the constituent elements (Merck AG: Ho and Y of 99.9% purity, Cu and Sn of 99.99% purity) under high-purity argon atmosphere on a water-cooled cooper hearth using titanium–zirconium alloy as a getter. In order to ensure good homogeneity the buttons were remelted several times. Subsequently, samples were annealed in an evacuated quartz tube at 800 °C for one week. The quality of the products was checked by x-ray powder diffraction at a temperature of 300 K. The analyses of the x-ray patterns indicate that all of the samples have the orthorhombic crystal structure of the $Gd_3Cu_4Ge_4$ type. No additional impurity phases were detected.

The magnetic properties were studied in the 2–300 K temperature range and in external magnetic fields up to 5 T employing an MPMS SQUID magnetometer. Specific heat studies were carried out in the 2–300 K temperature range by a quasi-adiabatic method using a Quantum Design PPMS platform. Neutron diffraction measurements were performed at the E6 diffractometer installed at the BER-II research reactor (BENSC-HMI). The specimens with mass of about 7 g were placed in cylindrical vanadium containers. Neutron diffraction patterns for $x = 1$ and 2 were collected within the 1.5–10 K temperature range with the incident neutron wavelength of 2.44 Å. Refinements of the neutron data were made using the Rietveld-type FullProf software [21].

3. Results

3.1. Crystal structure

Crystal structures of samples were determined using the x-ray data at 300 K and neutron diffraction at 10 K. In the structure of $Gd_3Cu_4Sn_4$ type the rare earth atoms occupy two different crystallographic 2d and 4e positions; Cu atoms are placed at the 8n position and the Sn atoms occupy the 4f and 4h positions. The analyses of these data allowed us to determine the Ho and Y atom preferences in occupying both sites. This was possible from the x-ray data only (Z is equal to 39 for Y and 69 for Ho). In the case of neutron diffraction the differences between scattering lengths are too small for reliable preferred occupation analysis ($b = 7.75$ fm for Y and 8.44 fm for Ho).

Table 1. Crystal properties of $Ho_{3-x}Y_xCu_4Sn_4$ compounds as derived from x-ray diffraction data. Calculated interatomic distances are labelled according to figure 1 ($A = R_{\mathrm{Ho2d-Sn4h}}$; $B = R_{\mathrm{Ho2d-Cu8n}}$; $C = R_{\mathrm{Ho2d-Sn4f}}$; $D = R_{\mathrm{Ho4e-Sn4f}}$; $E = R_{\mathrm{Ho4e-Sn4h}}$; $F = R_{\mathrm{Ho2d-Cu8n}}$). Standard deviations are given in parenthesis.

Compound	$Ho_3Cu_4Sn_4$	$Ho_2YCu_4Sn_4$	$HoY_2Cu_4Sn_4$
a (Å)	14.5796(1)	14.5951(1)	14.6193(1)
b (Å)	6.90736(5)	6.91309(4)	6.92171(4)
c (Å)	4.41981(3)	4.42468(3)	4.42914(3)
V (Å^3)	445.08(1)	446.45(1)	448.18(1)
A (Å)	3.026(4)	3.025(4)	3.020(4)
B (Å)	3.558(6)	3.562(5)	3.559(5)
C (Å)	3.168(7)	3.170(6)	3.168(6)
D (Å)	3.100(6)	3.100(6)	3.099(6)
E (Å)	3.211(8)	3.220(8)	3.231(7)
F (Å)	3.153(6)	3.257(6)	3.305(6)

Crystal unit cell parameters for all investigated compounds derived from x-ray diffraction data are gathered together in table 1. In addition, unit cell volumes and some selected interatomic distances are given. With increasing Y content all lattice constants expand in a linear manner. The same holds for unit cell volumes. However, the distances within neighbouring crystal coordination of the 2d and 4e positions do not exhibit similar simple behaviour. Figure 1 shows coordination of the 2d and 4e positions, which are occupied by Ho and/or Y atoms. According to the best suited model, for the $Ho_2YCu_4Sn_4$ compound the Y atoms do not occupy the 2d position. They are statistically distributed into the 4e position together with Ho atoms (with ratio 1:1). Consequently, the 2d position is occupied only by Ho atoms. For the $HoY_2Cu_4Sn_4$ compound the 4e sublattice is occupied by Y atoms, while the Ho ones occupy the 2d position. The above observations are supported by analysis of interatomic distances of 2d and 4e surroundings. A comparison of the distances between nearest neighbours (A, B, C) of the 2d position yields a lack of significant changes in the whole $Ho_{3-x}Y_xCu_4Sn_4$ ($x = 0$, 1, 2) family. This is clear evidence that the 2d position is occupied by Ho atoms only. On the other hand, similar analysis of the 4e position's surroundings gives opposite results. Admittedly, the D distance does not change, but E and F bond lengths expand dramatically with Y content increase.

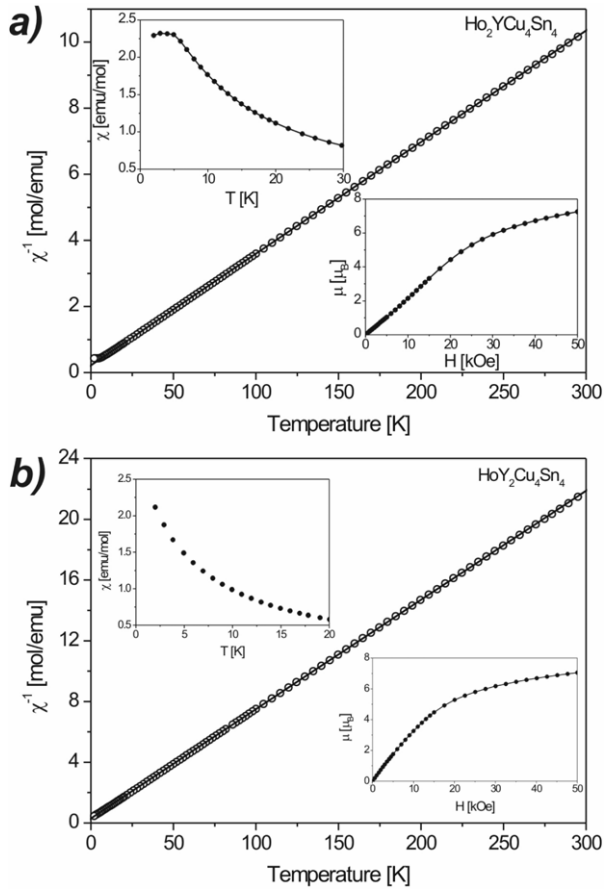

Figure 2. Temperature dependence of inverse magnetic susceptibilities of (a) $Ho_2YCu_4Sn_4$ and (b) $HoY_2Cu_4Sn_4$. The solid lines represent the Curie–Weiss law fits. The insets show the low temperature part of the magnetic susceptibility and Ho magnetic moment versus external magnetic field at 2 K.

3.2. DC magnetic susceptibility

The temperature dependences of magnetic susceptibilities and inverse magnetic susceptibilities for $x = 1$ and 2 are shown in figures 2(a) and (b), respectively. For both compounds magnetic susceptibilities follow the Curie–Weiss law with the paramagnetic Curie temperatures θ_p equal to $-6.47(4)$ K ($x = 1$) and $-4.16(4)$ K ($x = 2$). Refined effective magnetic moments μ_{eff} are equal to 10.92 μ_B ($x = 1$) and 10.95 μ_B ($x = 2$). The magnetic data for $Ho_3Cu_4Sn_4$ give the paramagnetic Curie temperature $\theta_p = 6.62(6)$ K and effective moments of 10.03(4) μ_B [18]. Magnitudes of θ_p parameters hint at lowering of the magnetic exchange strength with Y content increase.

For $x = 1$ a broad maximum is observed at about 5 K (see the inset to figure 2(a)), similar to those observed for $x = 0$ in the 4–8 K temperature range (see figure 1 in [18]). On the other hand, for $x = 2$ no evidence of a magnetic transition is visible (see figure 2(b)). The insets to figures 2(a) and (b) show the magnetization isotherms for both compounds at 2 K. For $Ho_2YCu_4Sn_4$ below $H = 5$ kOe the Ho magnetic moment is a linear function of the external magnetic field; moreover, the low slope of the curve is typical of antiferromagnetic behaviour. It is worth mentioning that the metamagnetic transition takes place at about 13 kOe. Similar behaviour was evidenced for the $Ho_3Cu_4Sn_4$ sample; however, the critical field was close to 20 kOe [18]. The difference is apparently connected to the lowering of magnetic coupling strength with increase of x parameter. At a field of 50 kOe no saturation can be observed; the Ho magnetic moment is equal to 7.3 μ_B. For $HoY_2Cu_4Sn_4$ the magnetization curve is typical of a paramagnetic substance. The Ho moment is equal to 7.5 μ_B at $H = 50$ kOe.

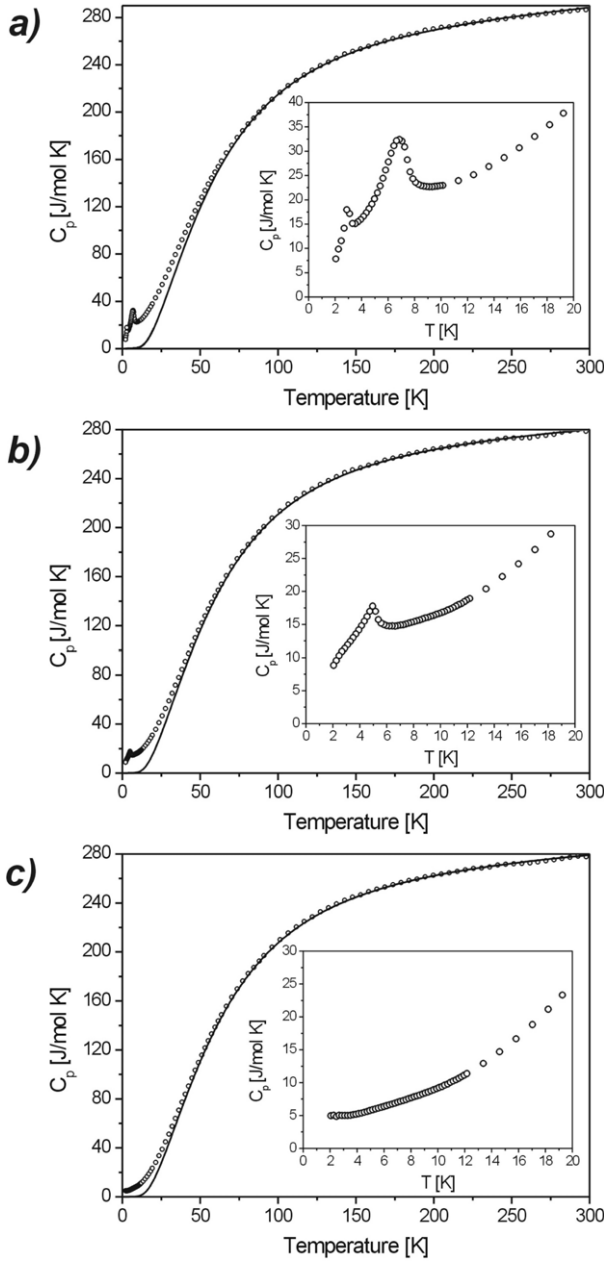

Figure 3. Temperature dependence of specific heat for (a) $Ho_3Cu_4Sn_4$, (b) $Ho_2YCu_4Sn_4$ and (c) $HoY_2Cu_4Sn_4$. The insets show the low temperature range of $C_p(T)$. The solid lines represent the sum of the lattice and electronic contributions.

3.3. Specific heat

In figure 3 specific heat versus temperature curves of the investigated compounds are presented. Magnetic phase transitions in the $Ho_3Cu_4Sn_4$ sample have been discussed in

Table 2. Characteristic temperatures, electronic and anharmonic coefficients derived for $Ho_{3-x}Y_xCu_4Sn_4$ compounds. Standard deviations are given in parenthesis.

	$Ho_3Cu_4Sn_4$	$Ho_2YCu_4Sn_4$	$HoY_2Cu_4Sn_4$
Θ_D (K)	201(3)	205(3)	212(4)
Θ_{E1} (K)	103(3)	102(2)	109(2)
Θ_{E2} (K)	168(4)	173(3)	178(4)
Θ_{E3} (K)	278(7)	281(6)	287(6)
γ (mJ mol^{-1} K^{-2})	24(2)	18(2)	14(2)
α (K^{-1})	$1.6(1) \times 10^{-4}$	$1.2(1) \times 10^{-4}$	$1.3(1) \times 10^{-4}$

detail elsewhere [18]. The recently collected new data are presented to be compared with other samples. The new data are analysed using other lattice and electron contributions. In [18] the lattice contribution was estimated taking into account the data for the non-magnetic Y-based analogue (with appropriate rescaling of the characteristic temperatures). However, it turned out that $Y_3Cu_4Sn_4$ could not be taken as a reference sample. When extracting the $Y_3Cu_4Sn_4$ data from the $HoY_2Cu_4Sn_4$ ones the estimated magnetic contribution was far higher than expected. An inset to figure 3(b) displays the low temperature behaviour of the $C_p(T)$ of $Ho_2YCu_4Sn_4$. A distinct anomaly at 4.9 K is a clear evidence of a transition into a magnetically ordered state. In contrast, for $HoY_2Cu_4Sn_4$ no such strong evidence of a magnetic transition could be observed (see the inset to figure 3(c)). However, according to the neutron diffraction results presented later, a slight rise of specific heat below 3 K is the onset of an anomaly due to magnetic ordering taking place at about 1.5 K.

The non-magnetic contribution to the specific heat was approximated using the following formula:

$$C_{\mathrm{ph+el}} = 9R\frac{1}{1-\alpha T}\left(\frac{T}{\Theta_D}\right)^3\int_0^{\frac{\Theta_D}{T}}\frac{x^4\mathrm{e}^x}{(\mathrm{e}^x-1)^2}\,\mathrm{d}x + R\frac{1}{1-\alpha T}\sum_i\frac{\left(\frac{\Theta_{Ei}}{T}\right)^2\mathrm{e}^{\frac{\Theta_{Ei}}{T}}}{\left(\mathrm{e}^{\frac{\Theta_{Ei}}{T}}-1\right)^2}+\gamma T \qquad (1)$$

where Θ_D is the Debye temperature, Θ_{Ei} are Einstein temperatures, γ is the electronic specific heat coefficient, α is the anharmonic coefficient and R is the gas constant. For both compounds there are three acoustic modes and 30 optical ones. The optical branches were grouped into three 'multiple' branches with multiplicity of 10. Such a rough estimation was applied to extract the magnetic part of the specific heat. Formula (1) was fitted to the experimental data above the temperature of 75 K. Obtained results are gathered in table 2. It is worth noting that the electronic contribution to the specific heat decreases when the Y content increases. This may be connected with lowering of RKKY interaction strength due to suppression of the density of states at the Fermi level. The above claim is supported by the fact that the absolute values of paramagnetic Curie temperatures become lower for higher Y content according to the above presented magnetometric data.

The magnetic contributions to the specific heat of investigated samples are presented in figure 4. The contribution arising from Schottky splitting of crystal field (CF) levels may

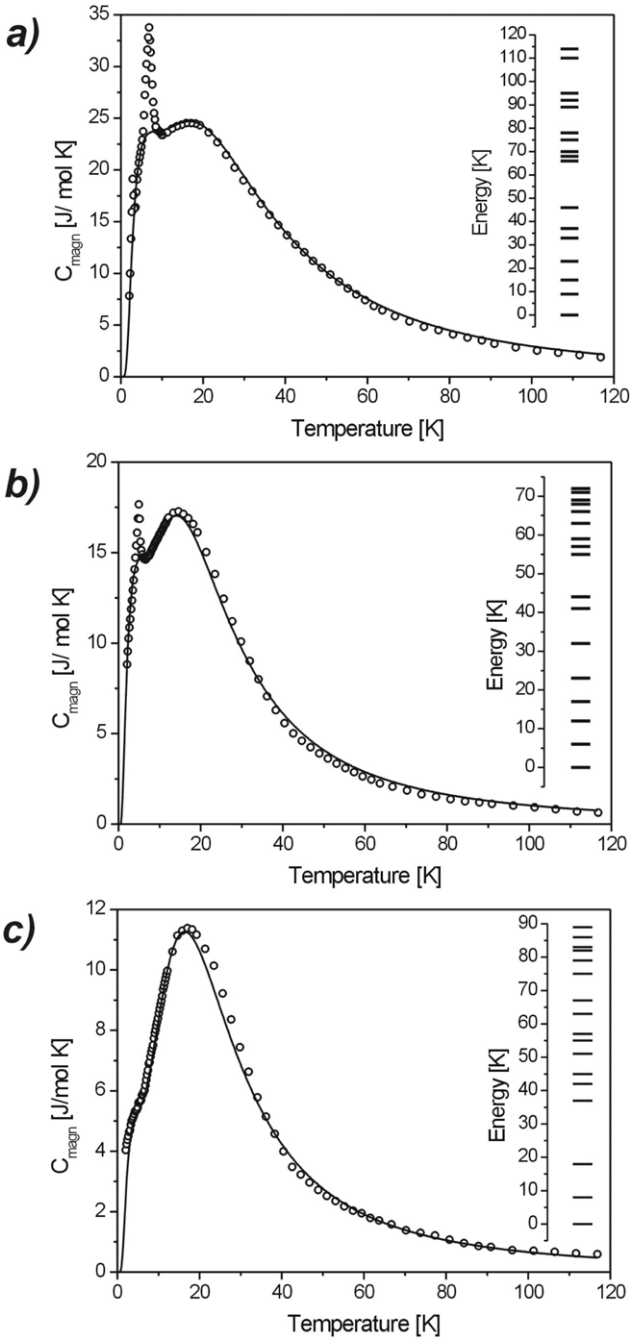

Figure 4. Magnetic contributions to the specific heat of (a) $Ho_3Cu_4Sn_4$, (b) $Ho_2YCu_4Sn_4$ and (c) $HoY_2Cu_4Sn_4$. The solid lines represent the Schottky contribution originating from crystal field splitting. The schemes of CF splitting are given in the inset to each diagram.

be described using the formula

$$C_{\mathrm{Schottky}} = \frac{nR}{T^2}\left[\frac{\sum_{i=1}^{17}E_i^2\mathrm{e}^{-\frac{E_i}{T}}}{\sum_{i=1}^{17}\mathrm{e}^{-\frac{E_i}{T}}}-\left(\frac{\sum_{i=1}^{17}E_i\mathrm{e}^{-\frac{E_i}{T}}}{\sum_{i=1}^{17}\mathrm{e}^{-\frac{E_i}{T}}}\right)^2\right] \qquad (2)$$

where the E_i parameters are the energies of CF levels (in Kelvin) and n is the number of holmium ions per formula unit. Due to the point symmetries of both Ho sites within the unit cell a set of nine parameters of the CF Hamiltonian

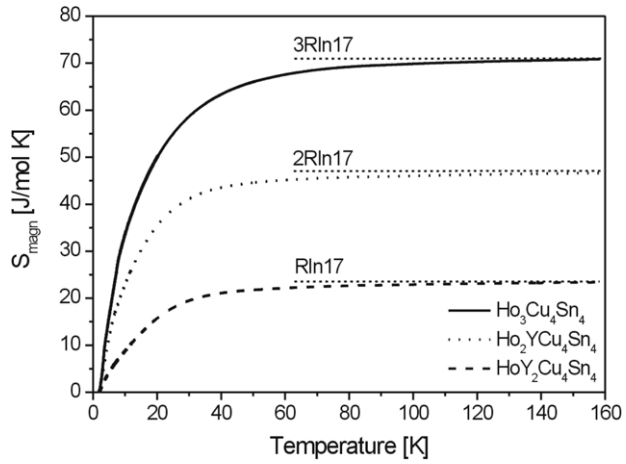

Figure 5. Magnetic entropy of investigated compounds as a function of temperature. Theoretical limits are marked with dotted lines.

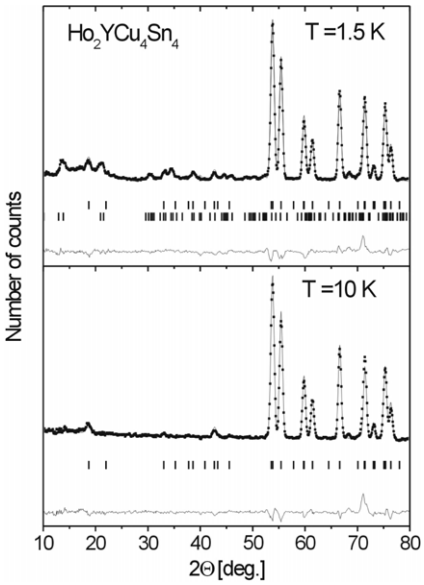

Figure 6. Neutron diffraction patterns of $HoY_2Cu_4Sn_4$ at 1.5 K (upper pattern) and 10 K (bottom pattern) together with Rietveld fits and difference plots. Vertical ticks indicate the positions of Bragg reflections of nuclear and magnetic (upper pattern only) origin.

should be considered: B_2^0, B_2^2, B_4^0, B_4^2, B_4^4, B_6^0, B_6^2, B_6^4, B_6^6. In this case the ground multiplet of the non-Kramers Ho ion splits into 17 singlets. Fits of equation (2) to the magnetic part of the specific heat are given in figure 4 as solid lines. The corresponding CF level splitting schemes are given as insets to figure 4. Estimated splitting schemes should be finally confirmed by inelastic neutron scattering, at least for $HoY_2Cu_4Sn_4$, where Ho ions occupy one atomic position. A comparison of splitting schemes lets us conclude that overall splitting of CF levels in the case of the $Ho_2YCu_4Sn_4$ (figure 4(b)) sample is significantly lower than in the case of $Ho_3Cu_4Sn_4$ or $HoY_2Cu_4Sn_4$ (figures 4(a) and (c)). For $Ho_2YCu_4Sn_4$ it is equal to 72 K, while for $Ho_3Cu_4Sn_4$ it reaches 114 K. The energy separations between ground and first excited CF levels are equal to 6 and 8 K for $Ho_2YCu_4Sn_4$ and $HoY_2Cu_4Sn_4$ compounds respectively. For $Ho_3Cu_4Sn_4$ the refined value is equal to 9 K. If the ground CF level is an intrinsically non-magnetic singlet, the magnetic ordering relies on the exchange interaction strength with respect to the above mentioned separation [21]. In our case, the rise of the separation energy leads to suppression of ordering temperature of $HoY_2Cu_4Sn_4$ in comparison to $Ho_2YCu_4Sn_4$. For $HoY_2Cu_4Sn_4$ the onset of the anomaly at about 1.5 K is more pronounced in the magnetic part of the specific heat (figure 4(c)) at low temperatures than in the original data (figure 3(b)).

Based on the magnetic contribution to the specific heat, a magnetic entropy was calculated using the $S_{\mathrm{magn}}(T) = \int_0^T \frac{C_{\mathrm{magn}}(T')}{T'} \mathrm{d}T'$ formula for each of the investigated compounds (see figure 5). In all cases $S_{\mathrm{magn}}(T)$ saturates below 160 K with a good agreement with theoretical limits $3R\ \ln 17$, $2R\ \ln 17$ and $R\ \ln 17$for $Ho_3Cu_4Sn_4$, $Ho_2YCu_4Sn_4$ and $HoY_2Cu_4Sn_4$ respectively.

3.4. Magnetic structure

The neutron diffraction pattern of the $Ho_2YCu_4Sn_4$ sample recorded at 1.5 K indicates additional peaks of magnetic origin (see figure 6). A comparison of this pattern with that of $Ho_3Cu_4Sn_4$ measured at 1.5 K (see figure 7 in [4] and figure 10 in [18]) clearly indicates that the additional peaks correspond to the magnetic ordering in the 2d site, which is described by the wavevector $\mathbf{k} = (0, 1/2, 0)$. Within the crystal unit cell the sequence of magnetic moments is [++]. The Ho magnetic moment is equal to 9.4(5) μ_B and it is parallel to the b-axis. The Ho ions occupying the 4e sublattice together with the Y ones do not exhibit magnetic ordering. In the 15°–25° range of 2θ a broad maximum is observed. This is an apparent consequence of some short-range magnetic correlations within the magnetically disordered 4e sublattice. For the $Ho_2YCu_4Sn_4$ compound at a temperature of 1.5 K (figure 7) some additional peaks of very small intensities are observed. These peaks are present in the same positions as for $x = 1$. This result suggests that near this temperature magnetic ordering in the 2d sublattice is established. The similar positions of these reflections with respect to those evidenced in $Ho_2YCu_4Sn_4$ are indicative of similar magnetic order in both compounds with $x = 1$ and 2.

4. Conclusions

The results presented above show that $Ho_{3-x}Y_xCu_4Sn_4$ compounds exist for $x = 0$, 1 and 2 with the orthorhombic $Gd_3Cu_4Sn_4$ type of crystal structure. In this structure the rare earth atoms occupy two non-equivalent positions in the crystal unit cell. The lattice parameters increase with increasing yttrium content as the radius of the Y^{3+} ion (0.905 Å) is larger that in the case of Ho^{3+} (0.894 Å). Presented x-ray diffraction data indicate that the doped Y atoms prefer the 4e position.

Magnetic, specific heat and neutron diffraction data for $Ho_2YCu_4Sn_4$ and $HoY_2Cu_4Sn_4$ clearly show that antiferromagnetic order of the 2d sublattice with the propagation vector $\mathbf{k} = (0, 1/2, 0)$ is established in both cases.

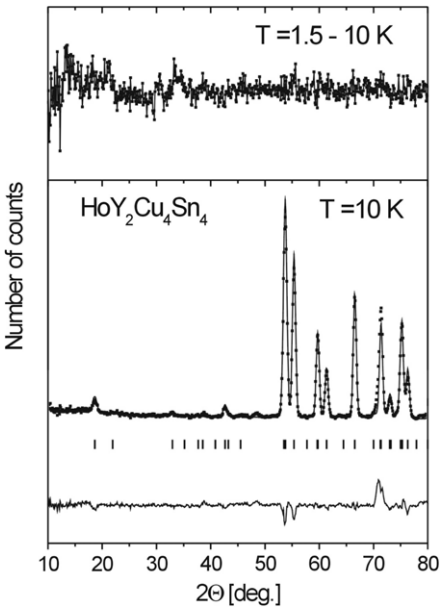

Figure 7. Neutron diffraction patterns of $HoY_2Cu_4Sn_4$ at 10 K (bottom pattern) together with Rietveld fits and difference plots and the 1.5–10 K difference (upper pattern).

The values of the Néel temperature decrease with increase of the x from 7.6 K for $x = 0$ [18] through 5.3 K for $x = 1$ down to 1.5 K for $x = 2$. The above mentioned behaviour may be related to the expansion of the unit cell leading to suppression of the exchange interaction. Apart from lowering of the ordering temperature, such a conclusion is supported by the evidenced decrease of the modulus of the paramagnetic Curie temperature.

Analysis of magnetic behaviour of the investigated $Ho_{3-x}Y_xCu_4Sn_4$ compounds suggests that ordering within the 2d sublattice is hardly affected by the presence or absence of magnetic ordering within the 4e sublattice.

Acknowledgments

This research project has been supported by the European Commission under the Sixth Framework Programme through the Key Actions Strengthening the European Research Area, Research Infrastructures. Contract No RII3-CT-2003-505925(NMI3).

Kind hospitality and financial support extended to two of us (SB and BP) by the Berlin Neutron Scattering Centre, Hahn–Meitner Institute, is gratefully acknowledged.

References

[1] Rieger W 1970 *Montash. Chem.* **101** 449–62
[2] Szytuła A, Wawrzyńska E, Penc B, Stüsser N and Zygmunt A 2003 *Physica* B **327** 167–70
[3] Wawrzyńska E, Hernandez-Velasco J, Penc B, Szytuła A and Zygmunt A 2003 *J. Magn. Magn. Mater.* **264** 192–201
[4] Wawrzyńska E, Hernandez-Velasco J, Penc B, Sikora W, Szytuła A and Zygmunt A 2003 *J. Phys.: Condens. Matter* **15** 5279–96
[5] Wawrzyńska E, Hernandez-Velasco J, Szytuła A and Zygmunt A 2003 *J. Alloys Compounds* **350** 68–71
[6] Wawrzyńska E, Penc B, Stüsser N, Szytuła A and Tomkowicz Z 2003 *Solid State Commun.* **126** 527–30
[7] Ryan D H, Cadogan J M, Cadogan R and Swaison I P 2004 *J. Phys.: Condens. Matter* **16** 3183–98
[8] Wawrzyńska E, Hernandez-Velasco J, Penc B, Szytuła A and Tomala K 2004 *J. Phys.: Condens. Matter* **16** 7535–44
[9] Wawrzyńska E, Hernandez-Velasco J, Penc B and Szytuła A 2004 *J. Phys.: Condens. Matter* **16** 45–52
[10] Szytuła A, Wawrzyńska E, Penc B, Stüsser N, Tomkowicz Z and Zygmunt A 2004 *J. Alloys Compounds* **367** 224–9
[11] Wawrzyńska E, Hernandez-Velasco J, Penc B, Rams R and Szytuła A 2005 *J. Magn. Magn. Mater.* **288** 111–20
[12] Wawrzyńska E, Hernandez-Velasco J, Penc B and Szytuła A 2005 *J. Magn. Magn. Mater.* **280** 234–42
[13] Mazzone D, Riani P, Napoletano M and Canepa F 2005 *J. Alloys Compounds* **387** 15
[14] Perry L K, Ryan D H, Canepa F, Napoletano M, Mazzone D, Riani P and Cadogan J M 2006 *J. Appl. Phys.* **99** 08J502(3)
[15] Wawrzyńska E 2005 *PhD Thesis* Jagiellonian University, Kraków
[16] Perry L K, Cadogan J M, Ryan D H, Canepa F, Napoletano M, Mazzone D and Riani P 2006 *J. Phys.: Condens. Matter* **18** 57–83
[17] Gondek Ł, Szytuła A, Kaczorowski D, Prokhnenko O and Nenkov K 2007 *Phase Transit.* **80** 563–73
[18] Gondek Ł, Szytuła A, Kaczorowski D, Szewczyk A, Gutowska M and Prokhnenko O 2007 *Intermetallics* **15** 583–92
[19] Gondek Ł, szytuła A, Kaczorowski D, Szewczyk A, Gutowska M and Piekarz P 2007 *J. Phys.: Condens. Matter* **19** 246225
[20] Singh S, Dhar S K, Manfrinetti P and Palenzona A 2000 *J. Alloys Compounds* **298** 68–72
[21] Trammel G T 1963 *Phys. Rev.* **31** 3625